

Examination of Artifacts from Multiband Imaging

Benjamin B. Risk^{ab}
Joint work with Daniel B. Rowe^c

^a Statistical and Applied Mathematical Sciences Institute, Research Triangle Park, NC 27709, USA

^b Department of Biostatistics, University of North Carolina at Chapel Hill, Chapel Hill, NC 27599, USA

^c Department of Mathematics, Statistics, and Computer Science, Marquette University, Milwaukee, WI 53233

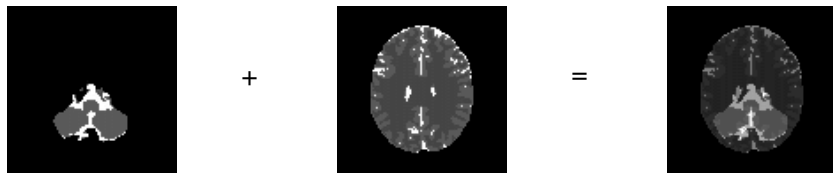
SAMSI Transitions Workshop, May 5, 2016

Outline of this talk

- Overview of multiband (MB) acquisition and head coils.
- Describe Slice-GRAPPA reconstruction.
- Previous research on costs and benefits of MB, gaps in research.
- Our simulation results examining impacts of MB on power and type 1.
- Example using task fMRI in the Human Connectome Project.

Multiband imaging

- We previously heard about in-plane acceleration, which can be used to increase spatial resolution.
- Through-plane acceleration, or *Multiband imaging*, can be used to increase temporal resolution.
- Simultaneously collect multiple slices, leading to a series of *packets*.
- Maximize the space between concatenated slices.
- Locations that are concatenated to form a single location are called *aliased*.



Costs and benefits of MB

- Shorter TR \implies more volumes, could lead to higher power.
- Unlike in-plane, no \sqrt{A} -penalty on the error because no lines of k-space are skipped.
- However, there may be error introduced when packets are separated.
- In particular, reconstruction introduces error such that signal in one voxel may leak to its aliased locations. Called *signal leakage* or *slice leakage*.
- Additionally, shorter TR requires a smaller flip angle contributing to less contrast between white and gray matter.

Multichannel head coils

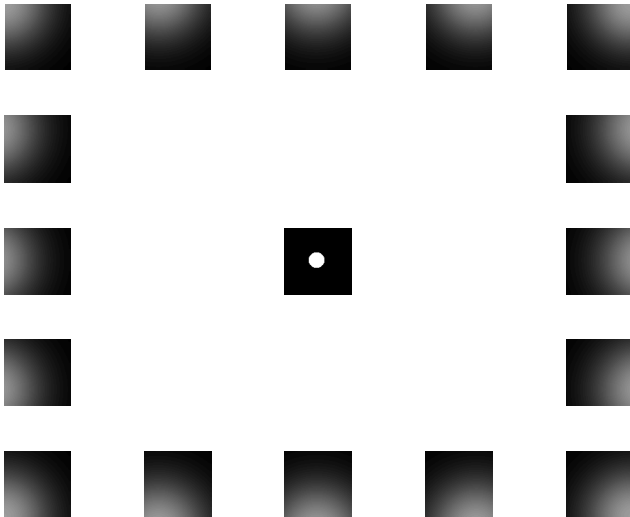
- Multi-channel head coils provide replication on the multislice packets which can be used to separate slices
- Huge data. Reconstruction online.

Source: <https://usa.healthcare.siemens.com>



Example Coil sensitivities

Axial z slice S to I 64 of 64



Re-construction using Slice-GRAPPA

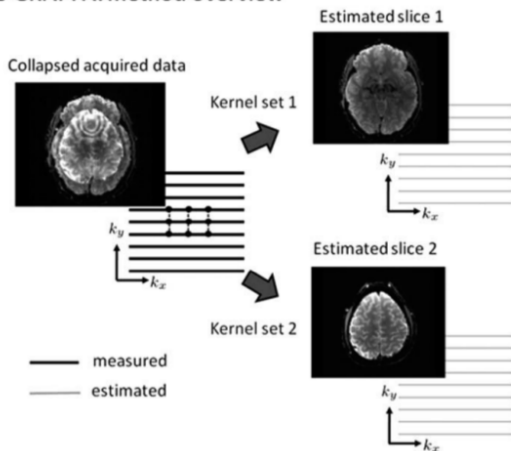
- GRAPPA reconstructs single-band data for each coil in k-space.
- Start with single-band calibration data from a single timepoint.
- Single-band data artificially collapsed to mimic multi-band data.
- A *kernel* is estimated, which is a set of weights of nearby spatial frequencies.

Slice-GRAPPA Overview

Figure : From Figure A3a, [Setsompop et al., 2012].

NOTE: Kernel (coefficients) estimation and reconstruction in kspace.

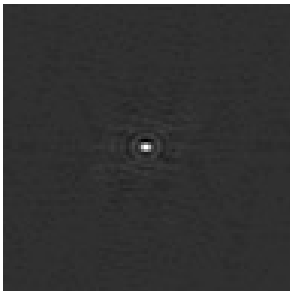
slice-GRAPPA: method overview



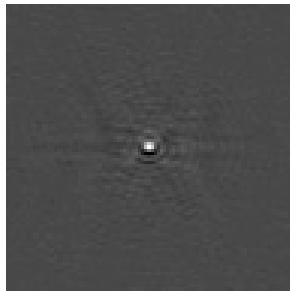
Slice-GRAPPA Overview

Figure : Collapsed k-space slice.

Real



Imaginary



Slice-GRAPPA calibration model

- Single acquisition volume (no time replication).
- $c \in \{1, \dots, C\}$ index coil.
- $k_y \in \{1, \dots, Y\}$ and $k_x \in \{1, \dots, X\}$ index the frequencies in the phase-encoding and read-out directions.
- Let $z \in \{1, \dots, Z\}$ denote a slice in single-band space.
- Let $S_{ck_y k_x z 0}^K \in \mathbb{C}$ denote k-space data.
- Let $m \in \{1, \dots, Z/A\}$ index the packet.
- $M_{ck_y k_x m 0}^K \in \mathbb{C}$ denote the packet data.
-

$$S_{ck_y k_x z 0}^K = \sum_{h=1}^C \sum_{i=-I}^I \sum_{j=-J}^J \eta_{chjiz} M_{h, k_y-j, k_x-i, m, 0}^K + \epsilon_{ck_y k_x z 0} \quad (1)$$

where $\text{Real}(\epsilon_{ck_y k_x z 0}) \sim \mathcal{N}(0, \sigma_{CZ, R}^2)$ and
 $\text{Imag}(\epsilon_{ck_y k_x z 0}) \sim \mathcal{N}(0, \sigma_{CZ, I}^2)$.

Estimating Slice-GRAPPA weights

- Note: With two-neighbor kernel, same 25 coefficients used for all spatial frequencies in a given slice for a given focal-coil by predicting-coil pair.
- Results in 25×32 coefficients for each coil of 72 slices = $25 \times 32 \times 32 \times 72 = 1,843,200$ coefficients.
- Estimated using complex-valued least squares.

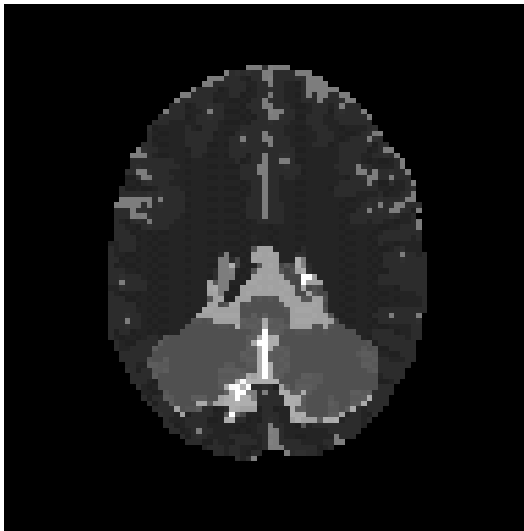
Reconstruction

- Apply coefficients to packet data for each TR in fMRI:

$$\hat{S}_{ck_y k_x zt}^K = \sum_{h=1}^C \sum_{i=-I}^I \sum_{j=-J}^J \hat{\eta}_{chjiz} M_{h,k_y-j,k_x-i,m,t}^K \quad (2)$$

- Inverse Fourier transform.
- Combine predictions for each coil using rms.
- Results in induced correlations and signal leakage (described later).

Aliased locations

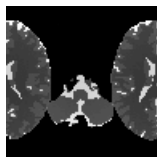


Blipped CAIPI for improved separation

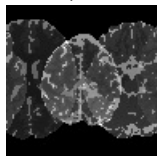
- Idea: Decrease overlap between collapsed slices by exploiting unused portions of the field of view.
- Controlled aliasing in parallel imaging (CAIPI)* using phase-shifts [Setsompop et al., 2012].
- Example: for the second slice of a packet with FOV/3:

$$S_{c_k y k_x z t}^{*K} = S_{c_k y k_x z t}^K e^{-i(k_y - 1)4\pi/3}.$$

MB = 2



MB = 4, FOV/3



Previous Work

- [Todd et al., 2016] evaluated empirical variants of sensitivity and false positives for different MB factors. Also evaluated an alternative reconstruction algorithm that was found to reduce leakage.

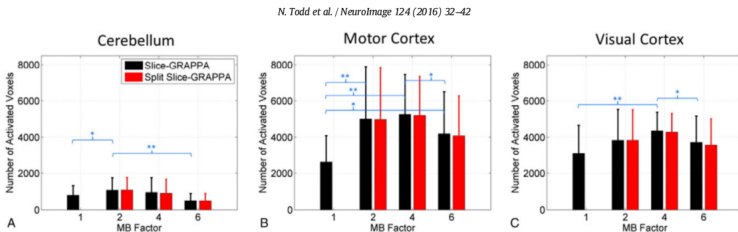


Fig. 4. Sensitivity analysis: number of activated voxels. The bar plots show the number of activated voxels within an anatomical region of interest that passed the significance threshold corresponding to $p < 0.001$, uncorrected (mean and standard deviation over all volunteers). Significant differences between the MB factors are shown in blue text, with * a significance level of $p < 0.05$ and ** a significance level of $p < 0.01$. There were no significant differences between the reconstruction types.

Previous work, cont.

38

N. Todd et al. / NeuroImage 124 (2016) 32–42

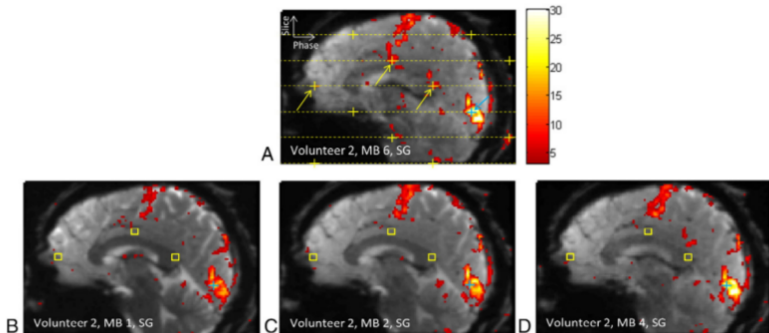


Fig. 6. Example of false-positive activation due to signal leakage between simultaneously excited slices. The top image shows the suspected false-positive activation from an MB 6 scan of Volunteer 2 with Slice-GRAPPA (SG) reconstruction, originating from the voxel at the blue cross and aliasing into voxels at the yellow arrows. The horizontal dashed yellow lines indicate the six slices that were simultaneously excited and acquired with the blue cross slice. The yellow crosses indicate the alias locations due to the combined CAIPI shift of FOV/3 and in-plane GRAPPA 2. The bottom row of images shows the MB 1, MB 2, and MB 4 results from the same volunteer. No activation is seen within a $3 \times 3 \times 3$ voxel ROI around the suspected false-positive locations from the MB 6 scan (yellow boxes). These three regions of activation from the MB 6 scan were therefore deemed to be false-positive activations.

Previous work, cont.

- Conclusions from [Todd et al., 2016]:
 1. MB 4 appeared to be more sensitive with fewer false positives.
 2. MB 6 had a lot of false positives. An alternative reconstruction algorithm reduced FPs.
 3. Recommended MB 2 with in-plane 2

Determination of HCP acquisition protocol

- Two papers contain information on the MB factors evaluated for use in the HCP, [Uğurbil et al., 2013] and [Xu et al., 2013].
- A third paper, [Smith et al., 2013], contains information on the protocol chosen for HCP.
- Propose measures of slice leakage but difficult to interpret.
- Suggest MB factor of 8 acceptable.
- From [Xu et al., 2013] p. 997-8:

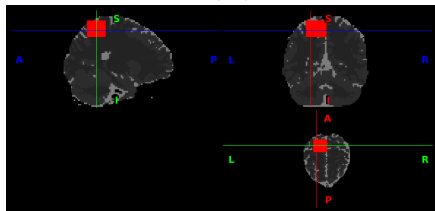
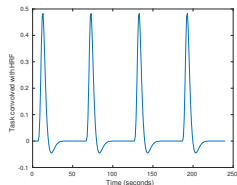
We can empirically consider a mean L-factor ≤ 0.05 and maximum L-factor ≤ 0.9 acceptable. Caution should be noted, however, in that these L-factors, stated as “acceptable”, are arbitrarily defined as an upper limit based on the integrity of previous fMRI experiments that demonstrate the expected spatial distributions and reliability in the functional maps. Additional rigorous fMRI analyses are needed to define more generalizable L-factor thresholds.

Our Simulation Study

- Simulate a localization study.
- 3-by-2 factorial design:
 - MB = 1, 4, 8
 - Caipi = None or FOV/3
- Scan time = 240 sec;
 - MB = 1: TR = 8 sec;
 - MB = 8: TR = 1 sec.
- 32 coils, 96 x 96 x 64 2.5 mm voxels, two-ring head coil.
- IID normal noise added to packets for each coil:

$$\sigma_R^2 = \sigma_I^2 = 1/\sqrt{2}.$$
- Create an activated region:

$$\beta \in \{0.01, \dots, 5\}.$$

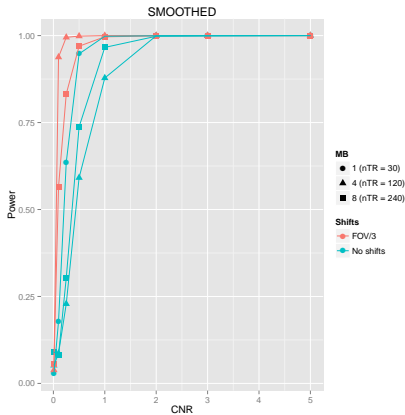
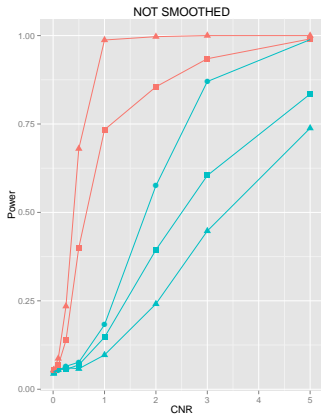


- Fit with SPM 12.
Non-smoothed and smoothed (7.5 x 7.5 x 7.5).

Examining Power

- With higher MB, we get more data. Does this increase power?
- With caipi shifts, we may get better reconstruction; does this increase power?

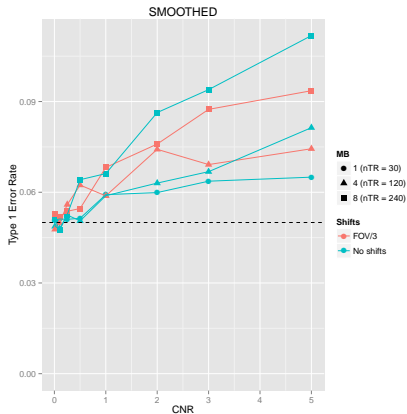
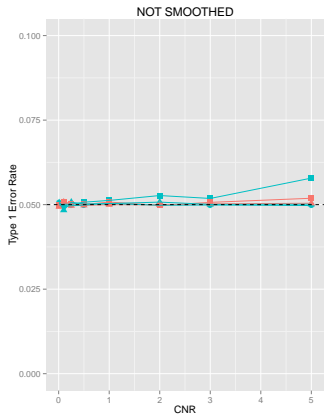
Simulations: Power



Examining False Positives

- With higher MB, we may get more leakage. Does this increase false positives?
- Do CAIPI-shifts decrease false positives?

Simulations: Type 1 Errors



Aliased locations: No Shifts

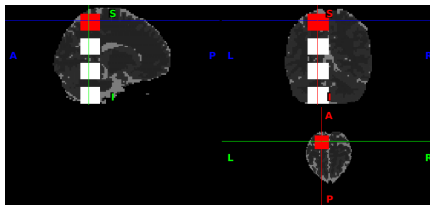


Figure : MB 4 with no caipi shifts

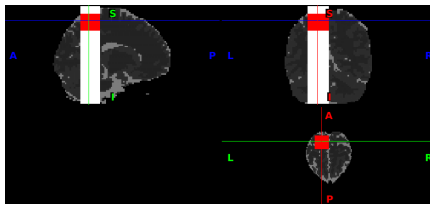


Figure : MB 8 with no caipi shifts.

Aliased locations: Caipi-Shifts

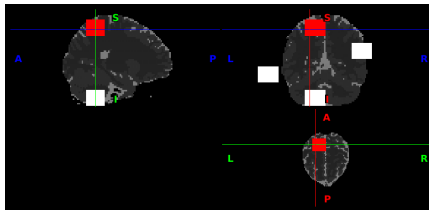


Figure : MB 4 with FOV/3 caipi shifts

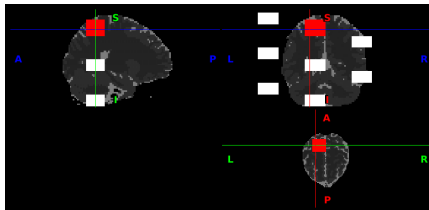
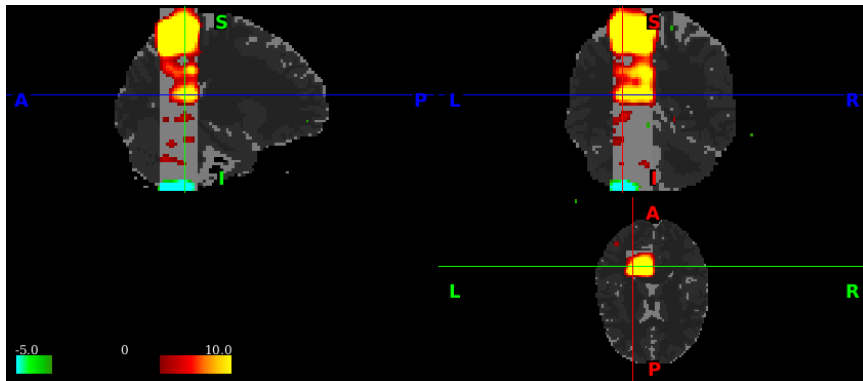
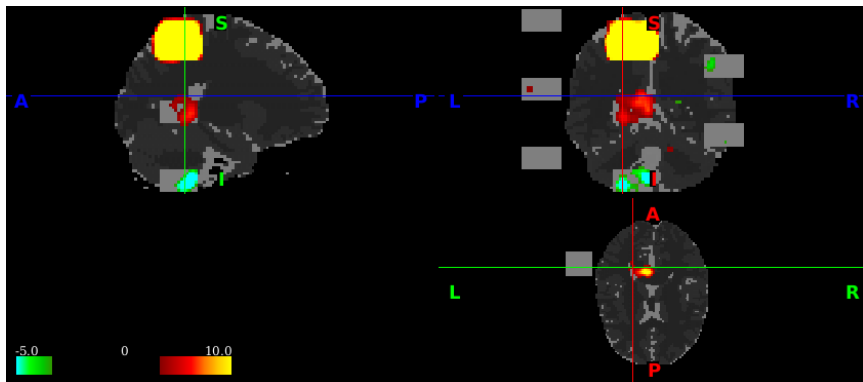


Figure : MB 8 with FOV/3 caipi shifts.

Simulations: MB=8 with no caipi and $\beta = 3$



Simulations: MB=8 with caipi and $\beta = 3$



HCP Data

- Human Connectome Project has made “unprocessed” and preprocessed data publicly available for hundreds of subjects.
- State-of-the-art scanners with gradients that can achieve very high acceleration factors.
- Use MB=8 and FOV/3, 32 channel head coil [Smith et al., 2013].
- Ordinary scanners may not be able to achieve this MB factor.

HCP Analysis

- Analyzed one session (RL) motor task from “unprocessed data” using SPM with no motion correction and FWHM = $6 \times 6 \times 6$ (three times voxel dimensions) for two subjects (100307 and 101915).
- Examined contrast between left hand and other tasks.
- Caveat: we did not analyze the processed data.
- Difficult to determine aliased locations in HCP minimally preprocessed data which uses “grayordinates.”
- Caveat: HCP minimally preprocessed data include less smoothing and thus are expected to have fewer false positives than our analysis.

Slice Leakage in 100307

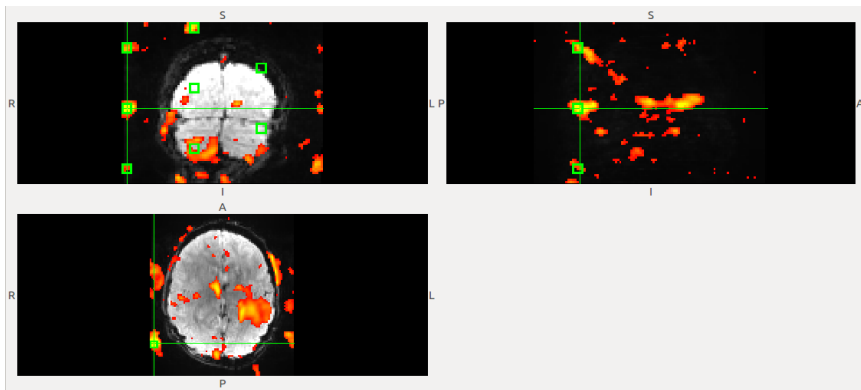


Figure : T-statistics of the left-hand contrast in subject 100307. The location of the crosshairs was chosen to illustrate apparent slice leakage. A 2-voxel neighborhood was created around the voxel located at the crosshairs, and green boxes depict the predicted aliased locations. Thresholded at $p < 0.05$ uncorrected.

Slice Leakage in 100307

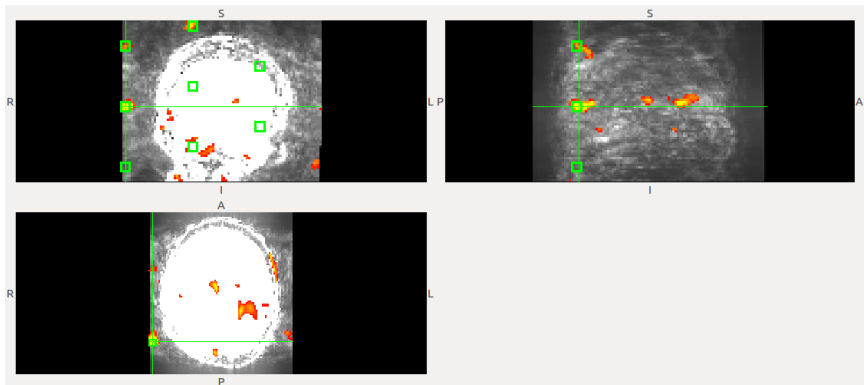


Figure : T-statistics of the left-hand contrast in subject 100307. The location of the crosshairs was chosen to illustrate apparent slice leakage. A 2-voxel neighborhood was created around the voxel located at the crosshairs, and green boxes depict the predicted aliased locations. Thresholded at $p < 0.001$ uncorrected.

Potential slice leakage in 101915

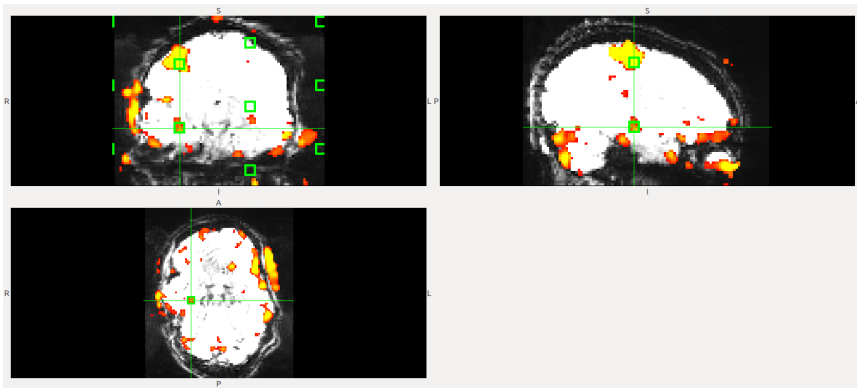


Figure : T-statistics of the left-hand contrast in subject 101915. The location of the crosshairs was chosen to illustrate potential slice leakage from the motor cortex. A 2-voxel neighborhood was created around the voxel located at the crosshairs, and green boxes depict the predicted aliased locations. Thresholded at $p < 0.001$ uncorrected. Note the aliased location may reflect real activation, activation induced by slice leakage, or small activation augmented by slice leakage.

Discussion

- There are benefits (more data) and costs (lower quality with slice leakage) to MB imaging.

Discussion

- There are benefits (more data) and costs (lower quality with slice leakage) to MB imaging.
- In simulations, MB 4 with caipi outperformed MB 8 both with respect to higher power and lower false positives.

Discussion

- There are benefits (more data) and costs (lower quality with slice leakage) to MB imaging.
- In simulations, MB 4 with caipi outperformed MB 8 both with respect to higher power and lower false positives.
- Note that adding more data does not improve reconstruction. With more time points, we actually increase the ability to detect signal leakage and incorrectly conclude activation.

Discussion

- There are benefits (more data) and costs (lower quality with slice leakage) to MB imaging.
- In simulations, MB 4 with caipi outperformed MB 8 both with respect to higher power and lower false positives.
- Note that adding more data does not improve reconstruction. With more time points, we actually increase the ability to detect signal leakage and incorrectly conclude activation.
- This is distressing.

Discussion

- There are benefits (more data) and costs (lower quality with slice leakage) to MB imaging.
- In simulations, MB 4 with caipi outperformed MB 8 both with respect to higher power and lower false positives.
- Note that adding more data does not improve reconstruction. With more time points, we actually increase the ability to detect signal leakage and incorrectly conclude activation.
- This is distressing.
- HCP uses a very high MB factor, and there is evidence of slice leakage and false activation.

Discussion

- There are benefits (more data) and costs (lower quality with slice leakage) to MB imaging.
- In simulations, MB 4 with caipi outperformed MB 8 both with respect to higher power and lower false positives.
- Note that adding more data does not improve reconstruction. With more time points, we actually increase the ability to detect signal leakage and incorrectly conclude activation.
- This is distressing.
- HCP uses a very high MB factor, and there is evidence of slice leakage and false activation.
- Our results suggest little is gained from very high MB factors, which was also found in [Todd et al., 2016]. These findings may vary with hardware and coil sensitivities.

Acknowledgments

Thank you to Mary Kociuba for helpful discussions. Data were provided (in part) by the Human Connectome Project, WU-Minn Consortium (Principal Investigators: David Van Essen and Kamil Ugurbil; 1U54MH091657) funded by the 16 NIH Institutes and Centers that support the NIH Blueprint for Neuroscience Research; and by the McDonnell Center for Systems Neuroscience at Washington University. This material was based upon work partially supported by the NSF grant DMS-1127914 to the Statistical and Applied Mathematical Science Institute.

References I



Setsompop, K., Gagoski, B. A., Polimeni, J. R., Witzel, T., Wedeen, V. J., and Wald, L. L. (2012).

Blipped-controlled aliasing in parallel imaging for simultaneous multislice echo planar imaging with reduced g-factor penalty.

Magnetic Resonance in Medicine, 67(5):1210–1224.



Smith, S. M., Beckmann, C. F., Andersson, J., Auerbach, E. J., Bijsterbosch, J., Douaud, G., Duff, E., Feinberg, D. A., Griffanti, L., Harms, M. P., et al. (2013).

Resting-state fmri in the human connectome project.

Neuroimage, 80:144–168.



Todd, N., Moeller, S., Auerbach, E. J., Yacoub, E., Flandin, G., and Weiskopf, N. (2016).

Evaluation of 2d multiband epi imaging for high-resolution, whole-brain, task-based fmri studies at 3t: Sensitivity and slice leakage artifacts.

NeuroImage, 124:32–42.



Uğurbil, K., Xu, J., Auerbach, E. J., Moeller, S., Vu, A. T., Duarte-Carvajalino, J. M., Lenglet, C., Wu, X., Schmitter, S., Van de Moortele, P. F., et al. (2013).

Pushing spatial and temporal resolution for functional and diffusion mri in the human connectome project.

Neuroimage, 80:80–104.



Xu, J., Moeller, S., Auerbach, E. J., Strupp, J., Smith, S. M., Feinberg, D. A., Yacoub, E., and Uğurbil, K. (2013).

Evaluation of slice accelerations using multiband echo planar imaging at 3t.

Neuroimage, 83:991–1001.